Extended Abstracts of the 2002 International Conference on Solid State Devices and Materials, Nagoya, 2002, pp. 730-731

B-9-2

Investigation of the Ti-Doped Ta_2O_5 Films from PET and TET Cocktail Source for DRAM Capacitor

K.J. Nam, K.C. Kim, J.S. Lim, K.V. Lim, Y.S. Kim, S.T. Kim, U.I. Chung and J.T. Moon

Process Development Team, Semiconductor R&D Center, Samsung Electronics Co. Ltd.
San #24 Nongseo-Ri, Yongin, Kyungki-do 449-900, Korea
Phone: +82-31-209-6349 Fax: +82-31-209-6299 E-mail: namkjin@samsung.co.kr

1. Introduction

Ta_2O_5 has been studied intensively as a dielectric material for the next generation DRAM because of its higher dielectric constant in comparison to SiO_2 and Si_3N_4 as well as its compatibility with microelectronics. Recently, Cava *et al* have reported that the dielectric constant of bulk Ta_2O_5(TaO) can be increased from 35.4 to 126.2 by adding about 8 mol% of TiO_2[1]. Nielsen *et al* and Gan *et al.* have reported that the dielectric constant of Ti-doped Ta_2O_5 (TTO) film by sputtering can be increased from 22~40.6 to 38~54.7, respectively[2,3]. In addition, Jimenez *et al.* demonstrated the fabrication of the Ti-doped TaO films by MOCVD process using $Ta(OEt)_4$(DMAE) and $Ti(OEt)_2(MDAE)_2$ precursors[4]. In consequence, their results would extend the applicability of TaO capacitor to even higher density memory devices. In this paper, we have deposited Ti-doped TaO (TTO) films from a cocktail source which contains 92 mol% PET [$Ta(OC2H_5)_5$] and 8 mol% TET [$Ti(OC_2H_5)_4$]. The deposition properties and the electrical properties of TTO films were investigated.

2. Experimental

The advantage of using the cocktail source is that the conventional TaO hardware deposition system can be used by only replacing the PET source with the cocktail source. Before the deposition process, the thermal stability of cocktail source was analyzed by TG, DTA and NMR analyses. The PET and TET have similar chemical structure and vapor pressure, and as a result the cocktail source exhibited nearly identical properties to that of PET and TET. The process sequence for MIS (Metal-Insulator-Semiconductor) capacitor is as followed. (1) OCS (One Cylinder Stack) poly-Si bottom electrode, (2) 800℃ 60sec PH_3 doping, (3) 800℃ 3min NH_3 nitridation, (4) 460℃ 3torr dielectric deposition, (5) 700℃ 2min O_3 annealing, (6) 750℃ 30min Dry-O_2 annealing, (7) TiN 250Å top electrode, (8) plate poly Si deposition process.

3. Results and Discussion

Fig.1(a) and 1(b) show the atomic ratio of Ti in TTO film measured by TXRF (Total Reflection X-ray Fluorescence). Although the cocktail source contains 8 mol% TET and 92 mol% PET, the deposited film has only about 2.1 atom% of Ti. Fig.1(b) shows the repeatability of the doping concentration of Ti in TTO films during 510 wafers deposition. Fig.2 shows the deposition rate of TaO and TTO as a function of the deposition temperature. Both TaO and TTO films showed a similar activation energy according to the Arrhenius plot. The capacitor structure used in this paper is shown in Fig.3. The step coverage of TTO dielectric is about 95%. Fig.4 shows the Toxeq. (Equivalent Thickness) versus the leakage current of TTO and TaO films at the applied voltage of ±1.5V. In case of TaO, the leakage current abruptly increases from the point at Toxeq. 33Å. However, a sudden change of the leakage current at each bias voltage up to Toxeq. 30Å is not observed with the TTO capacitor. Fig.5 shows the TDDB (Time Dependence Dielectric Breakdown) characteristics of TaO (Toxeq. 35Å) and TTO (Toxeq. 31Å) capacitors under the constant voltage stress. The voltages satisfying the 10 year lifetime of TaO and TTO dielectrics are 3.1V and 2.6V at MTTF, respectively. Fig.6 shows the X-ray diffraction patterns of TaO and TTO films with various annealing temperatures. The crystallization of both dielectrics begin at 700℃, and the preferred orientations are the same for both TaO and TTO. The XPS spectra of Ta4F binding energy in TaO and TTO films from the as-deposited and 750℃-annealed films are shown in Fig.7. The change in the binding energy is similar within the analysis limit in both films.

To understand the leakage current behavior, bi-layered dielectric structures are fabricated in addition to the above analysis. Fig.8 shows the various bi-layered structures of capacitor dielectrics. After the deposition of the storage poly-Si and pre-treatment process, 20Å-thick TTO layer (initial TTO) was deposited, followed by the deposition of the final TTO layer (Fig.8(a)) or the final TaO layer (Fig.8(b)). In addition, another set of samples are prepared by first depositing 20Å-thick TaO (initial TaO), and the final layers are deposited with TTO layer (Fig.8(c)) or TaO layer (Fig.8(d)). Fig.9 shows the leakage current behavior according to each bi-layered structures in Fig.8. The structures with the initial layer of TTO film (Fig.8(a) and (b)) show a similar leakage current behavior regardless of the final dielectric layers. The structures with the initial TaO film (Fig.8(c) and (d)) also show a similar leakage current behavior regardless of the final dielectrics. Compared to the bi-layered structures having the initial TTO film, the bi-layered structures having the initial TaO film show a slightly increased Toxeq. and increased leakage current at the negative bias under -5MV/cm. From these results, it is thought that the initial Ti-doped layer during the bi-layered dielectric deposition process improves the negative leakage current characteristics by affecting the properties of the final dielectric deposition layer.

Fig.10 shows the schematic band diagram suggested from the above results. Since the barrier height between TiN top-electrode and TaO dielectric is very low, the leakage current under the negative bias voltage follows Schottky emission mechanism. The schottky barrier height is determined by the sum of the band bending due to the image force and the positive charges such as vacancies in dielectric film. The improvement of the negative leakage characteristics of the bi-layered structures with the initial TTO film is thought to have a lower positive charges compared to the initial TaO structured film. Finally, it is thought that the initial Ti-doped layer may cause the reduction of the positive charges and also reduce the charges in the final layer.

4. Conclusions

We fabricated Ti-doped TaO films by CVD using the cocktail source. TTO films with 2 atom% of Ti showed a stable leakage current properties at Toxeq. 30Å. TDDB characteristics of the TTO capacitor satisfied the 10 year lifetime. The role of Ti in improving the leakage current characteristics can be explained by the reduction of the positive charges in the whole layers of the dielectric.

References

[1] R. F. Cava, *et al.*, Nature, vol. 377(21), 215, 1995.
[2] M. C. Nielsen, *et al.*, IEEE Trans. Components. part B, vol. 21(3), 274, 1998.
[3] J. Y. Gan, *et al.*, Appl. Phys. Lett., 72(3), 332, 1998.
[4] C. Jimenez, *et al.*, J. Phys. IV France, 9, Pr8-569, 1999.

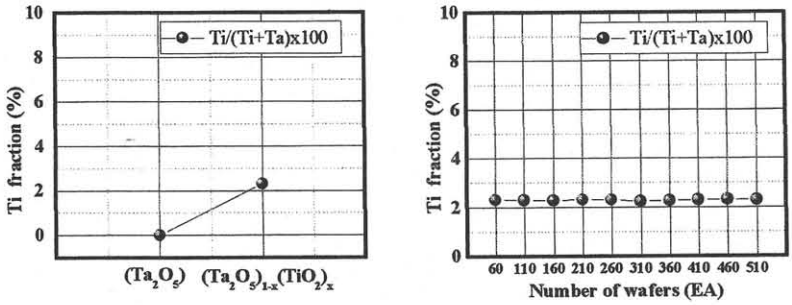

(a) (b)

Fig.1. (a) Ti concentration in Ta_2O_5 and $(Ta_2O_5)_{1-x}(TiO_2)_x$ films, (b) repeatability of Ti concentration in $(Ta_2O_5)_{1-x}(TiO_2)_x$ during 510 wafers deposition.

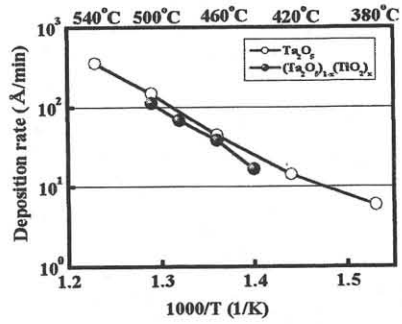

Fig.2 Arrhenius plot of $(Ta_2O_5)_{1-x}(TiO_2)_x$ and Ta_2O_5.

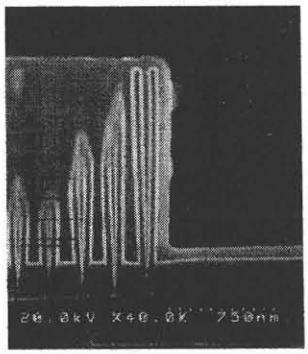

Fig.3 MIS capacitor structure. Aspect ratio≥25:1.

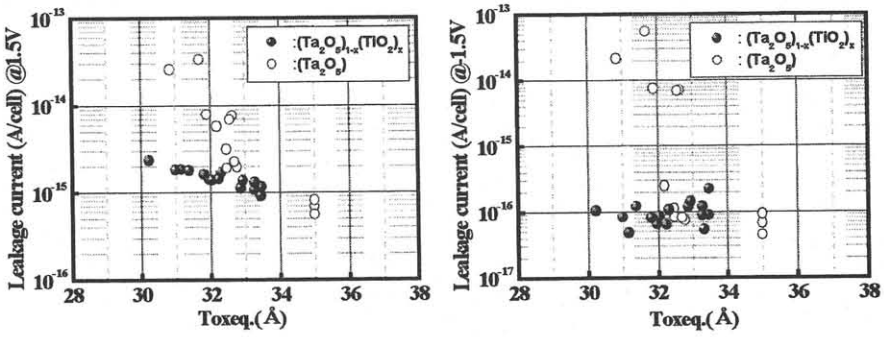

(a) (b)

Fig.4 Toxeq. vs. leakage current of Ta_2O_5 and $(Ta_2O_5)_{1-x}(TiO_2)_x$ capacitors at (a) +1.5V (b) -1.5V bias.

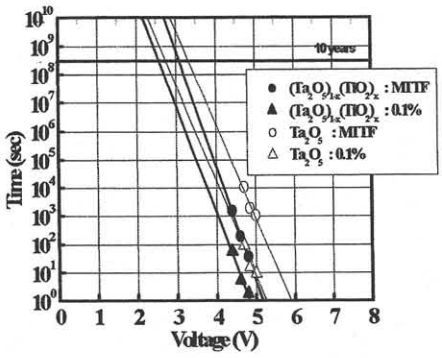

Fig.5 TDDB characteristics of Ta_2O_5 and $(Ta_2O_5)_{1-x}(TiO_2)_x$ capacitors.

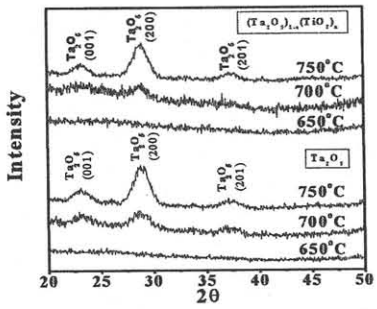

Fig.6 X-ray diffraction patterns of Ta_2O_5 and $(Ta_2O_5)_{1-x}(TiO_2)_x$ films with various annealing temperatures.

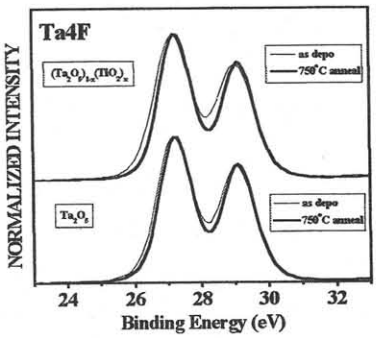

Fig.7 XPS spectra of Ta_2O_5 and $(Ta_2O_5)_{1-x}(TiO_2)_x$ films.

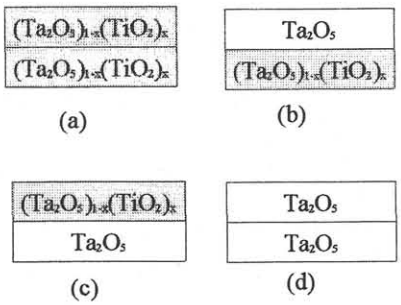

Fig.8 Various bi-layer test structures of capacitor dielectrics.

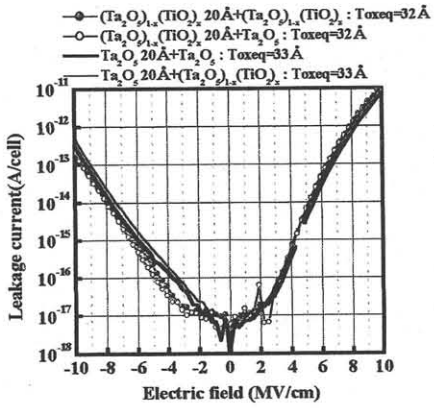

Fig.9 Leakage current curves and Toxeq. values from Fig.8 test structures.

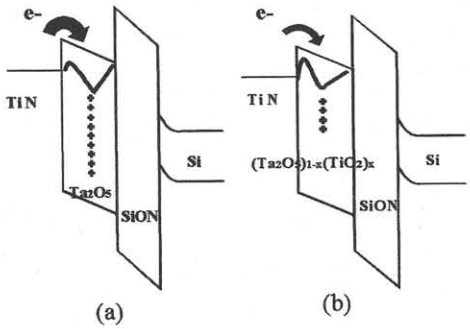

Fig.10 Schematic diagrams of electron emission under the negative bias (a) Ta_2O_5, (b) $(Ta_2O_5)_{1-x}(TiO_2)_x$